

## MULTI-HAZARD STOCHASTIC TIME-DEPENDENT TROPICAL CYCLONE FRAGILITIES FOR COASTAL STRUCTURES

ANDRES F. CALVO<sup>1</sup>, JAMIE E. PADGETT<sup>2</sup>

<sup>1</sup>Rice University  
6100 Main Street, 77005, Houston, TX  
[Andres.Calvo@rice.edu](mailto:Andres.Calvo@rice.edu)

<sup>2</sup> Rice University  
6100 Main Street, 77005, Houston, TX  
[Jamie.Padgett@rice.edu](mailto:Jamie.Padgett@rice.edu), <https://padgett.rice.edu/>

**Key words:** multi-hazard reliability, fragility model, tropical cyclones, stochastic, experimental-based power spectrum, industrial infrastructure

**Abstract.** *This study presents a methodology for derive multi-parameter fragilities for coastal structures subjected to multi-hazard tropical cyclone loads. The proposed analytical model generates multi-point stochastic time histories leveraging power spectrum informed by existing single hazard experimental data. A time dependent reliability analysis is performed in a quasi-static fashion to assess the extent of damage, progressive damage, cascading consequences and modification of the transferred loads from the envelope and structural systems. Surrogate models of multi-dimensional regression are used to derive close form fragilities. The proposed framework fills the gap between simplified and code-based multi-hazard load assessment and complex and expensive computational fluid dynamic multi-phase and multi-physics models. The portal frame structures typically found in industrial facilities located in coastal settings are used as a case study.*

## 1 INTRODUCTION

Multiple infrastructures, buildings and specialty structures are heavily exposed to the action of seasonal tropical cyclones in coastal settings around the world. This major natural disaster phenomenon is a multi-hazard event that combines extreme wind, waves, storm surge and rainfall. Extensive damage and losses have been experienced by the built environment during past TC events [1]. The industrial infrastructure has proven to be very vulnerable to these multi-hazard events reporting multi-million losses due to damage and loss of functionality (i.e., business interruption) [1], [2]. For example, industrial structures, such as the single-bay portal frame structures, sustain heavy damages to the envelope system (e.g., cladding panels, windows and doors), failure of secondary structural elements and collapse of entire bays. The combined action of wind, surge and wave derived in major damage to the envelope walls, extreme wind uplift produced multiple roof panels to fail, the water ingress due to surge and wave or rain lead to interior equipment damages [3], [4]. The repair and replacement costs must be added to the idle time and the business interruption losses. Therefore, the multi-hazard reliability assessment is necessary to account for the damage extent and failure probability of structures when subjected to multiple TC hazard stressors.

The reliability analysis of coastal structures subjected to these stressors represents a challenge due to the lack of multi-hazard data from past events, very limited experimental tests and scarcity of multi-hazard methodologies among other limitations [5], [6]. Additionally, high fidelity computational fluid dynamics (CFD) simulations for multi-phase multi-physics are very intensive on computational resources and difficult to validate. Therefore, combined single-hazard analysis is often preferred for regional risk assessment [1], [2], [3]. However, it results in an additional challenge to account for non-simultaneous peak pressures, spatial correlation/coherence determination [2], [4]. To overcome these issues heuristics such as the Sub-assembly approach [5] are used to determine lower and upper bounds for the independent and joint behavior [3], [6]. Additionally, simplify design-oriented methodologies such as the ones provided by standards (e.g., ASCE 7) are used to estimate conservative extreme value predictions [7]. Nevertheless, this led to overestimation of the loads and made it a challenge to measure uncertainty in the pressure patterns.

To overcome these limitations and fill the gap between existing analytical frameworks and complex CFD simulation, the present study proposes a new multi-hazard methodology to evaluate the reliability of envelope and structural systems in a time-dependent fashion by generating stochastic multi-point time history analysis. The multi-hazard time series are generated leveraging a spectral representation method that uses experimentally informed power spectrums to generate stochastic non-gaussian processes. The spatio-temporal analysis of multi-hazard stressors allows to account for spatially distributed pressures, progressive damage, loading path modifications, cascading effects such as internal pressurization and water ingress. Additionally, multiple geometries and properties can be incorporated into the analysis to represent heterogenous structural classes and heterogenous portfolio of structures. A smart Monte Carlo stopping rule is implemented to maximize the information of limited number of simulations while meeting a target level of confidence in the results.

## 2 METHODOLOGY FOR MULTI-HAZARD TC FRAGILITY

The proposed methodology is presented in Figure 1 and explained in detail in the following sections. The portal frame structures are used as a case study; however, the presented framework can be adapted to coastal building-like structures.

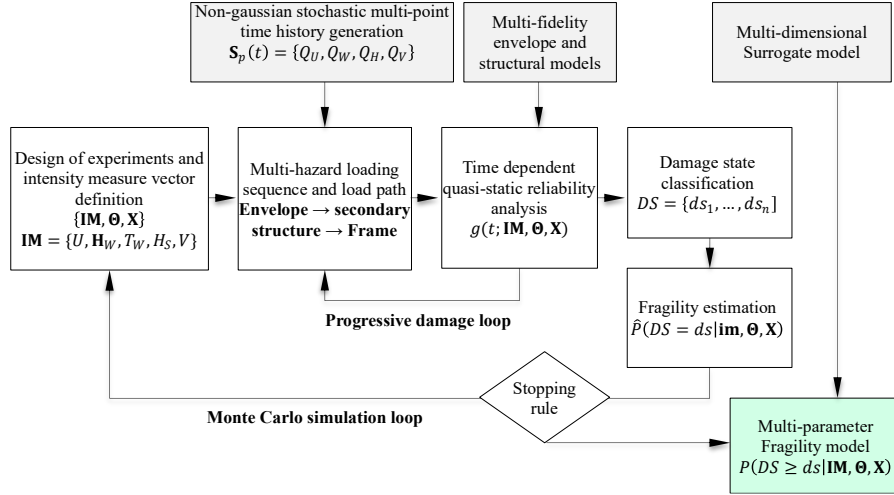


**Figure 1:** Proposed methodology for multi-hazard stochastic time dependent fragility assessment

### 2.1 Time dependent pressure generation

The multi-point time histories for the wind and wave pressure as well as the temporal evolution of the surge level are generated analytically. For wind and waves, experimental tests are used to inform power spectrums. The wind tunnel database for low-rise structures conducted by the Tokio Polythetic University was used for wind pressures [8]. For wave loads, the experimental tests on the wave funnel of Oregon University conducted by [9] were leveraged the was used to inform non-breaking and breaking waves pressures. Both databases contain time series of surface pressure at different points (pressure taps). The surge elevation was treated as a linear ramp from zero to  $H_s$  in time  $T_s$ .

The wind and waves power spectrums were used to generate multi-point stochastic time histories by means of a spectral representation method. The proper orthogonal decomposition (POD) was used considering its efficient algorithm implementation [10]. POD generates stochastic gaussian processes as presented in Eq.1. The eigenvalues and eigenvectors are calculated from the cross-spectral density matrix that contains the spatio-temporal correlation of the phenomena for the  $n$  points in the frequency domain. Another advantage of POD is the possibility of reconstructing a stochastic set of time histories using a few modal frequencies. Finally, POD can be used to generate time records beyond the experimental time window. Hence, multiple TC event durations  $T_e$  can be addressed. The stochastic representation propagates uncertainty in the wind and wave hazards records allowing the explicit evaluation of the performance of structures under TC loads. Thus, the same intensity measure (i.e., wind speed and wave height) is represented by multiple records.

$$S_p^{GP}(t) = \sum_{n=1}^{N_m} \sum_{j=1}^{N_\omega} 2|\Psi_p(\omega_n)|\sqrt{\Lambda_n(\omega)\Delta\omega} \cos(\omega_n t + \theta_p(\omega_n) + \phi_{pn}) \quad (1)$$

where  $S_p^{GP}(t)$  = Gaussian, zero mean time series at pressure tap  $p$ , the term  $|\Psi_p(\omega_n)|\sqrt{\Lambda_n(\omega)\Delta\omega}$  accounts for the modal decomposition with  $\Delta\omega$  = frequency increment with a cut-off frequency equals to  $N_\omega\Delta$ .  $\theta_p(\omega_n) = \tan^{-1}(\text{Im}[\Psi_p(\omega_n)]/\text{Re}[\Psi_p(\omega_n)])$  is the phase angle and  $\phi_{pn} = [0 - 2\pi]$  is a random value that introduces stochasticity.

The generated stochastic gaussian process can be then translated into a non-gaussian process by leveraging a direct translation approach or another method. Both the wind and waves display non-gaussian behavior. The direct transformation [11] is an efficient method to translate the process by using an arbitrary cumulative distribution function (cdf) as a mapping function from the standard normal cdf as shown in Eq.2.

$$S_p(t) = F_{S_p}^{-1} \left[ \Phi \left( \frac{S_p^{GP}(t) - E[S_p^{GP}(t)]}{\sqrt{\text{Var}[S_p^{GP}(t)]}} \right) \right] \quad (2)$$

where  $S_p(t)$  = non-Gaussian vector at pressure tap  $p$ ,  $F_{S_p}^{-1}[\cdot]$  = inverse cumulative distribution function (cdf) of an appropriate arbitrary continuous distribution,  $\Phi(\cdot)$  = standard Gaussian cdf corresponding to the standardization of the Gaussian process  $S_p^{GP}(t)$  with expected value  $E[S_p^{GP}(t)]$  and variance  $\text{Var}[S_p^{GP}(t)]$ .

## 2.2 TC multi-hazard demands

For TC winds, the non-gaussian process stochastically generated is the external pressure coefficient that is measured in wind tunnel tests at pressure taps locations (i.e.,  $S_p^{wind}(t) = C_e(t)$ ). Therefore, the wind velocity is treated as a deterministic intensity measure and the spatio-temporal variation is captured by the pressure coefficient. This way the wind pressure at any given point in the surface of the building can be computed as the velocity pressure shown in Eq.3.

$$Q_U^{(k)}(t; \mathbf{IM}, \boldsymbol{\Theta}, \mathbf{X}) = \frac{1}{2} \rho_a [U_{\bar{z}}(\mathbf{IM}, \mathbf{X})]^2 [C_e^{(k)}(t; \boldsymbol{\Theta}, \mathbf{X}) + C_i^{(k)}(t; \boldsymbol{\Theta}, \mathbf{X})] \quad (3)$$

where  $\rho_a$  = air density,  $U_{\bar{z}}(\mathbf{IM}, \mathbf{X})$  = projected wind speed at mid-roof level for the corresponding 3-s peak gust wind velocity  $U$  contained in  $\mathbf{IM}$  and building parameters  $\mathbf{X}$ .  $C_e^{(k)}(t; \boldsymbol{\Theta}, \mathbf{X})$  = dynamic external pressure coefficient acting on the  $k$ -th point in the structure's envelope generated considering the hazard parameters  $\boldsymbol{\Theta}$ . The aerodynamic wind forces  $F_U(t; \mathbf{IM}, \boldsymbol{\Theta}, \mathbf{X})$  correspond to the integration of all the pressures points within a determined tributary area. **Error! Reference source not found.** presents an external pressure coefficient time histories for multiple points in the envelope and the spatial pressure distribution at an instant.

For reliability applications, the wind is often treated probabilistically but time invariant. Therefore, it is necessary to evaluate the pressures for the envelope and structural system separately to account for joint peak pressures. Similarly, the existing design methodologies such as the one found in the ASCE 7, assume building zones with homogenous or very similar extreme pressures. Therefore it is not intended for analysis of spatio-temporal progression of

wind pressure loading. Another common application is using extreme theory to sample from the wind tunnel results those accounts for spatial distribution and aerodynamic interactions. However, the resulting pressure patterns lack a correlation structure and would be challenging to study the evolution of damage in a time dependent fashion. Thus, the present framework aims to evaluate the performance of the envelope and structural systems as the TC event unfolds.

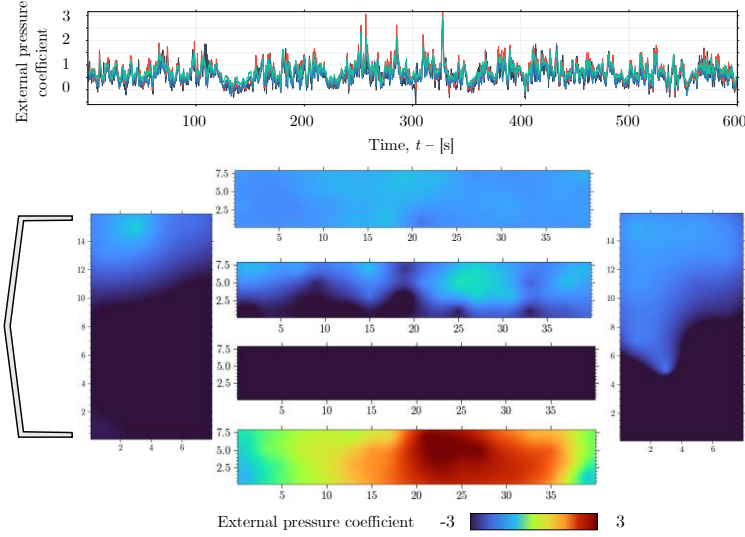


**Figure 2:** Proposed methodology for multi-hazard stochastic time dependent fragility assessment

Contrary to wind pressure, there is no analytical formulation to widely known wave pressure formulation for buildings as a function of the sea state at shoreline (i.e., wave height, period and fluid velocity) [1], [7], [12]. Therefore, the pressure profile cannot be analytically estimated from the existing wave power spectrums for shallow waters at shoreline in hurricane conditions such as the TMA, from which stochastic waves were generated [9]. For cylindrical offshore structures, the Morrison equations can be used to map the sea state to multi-point pressure at building surface [13]. Instead, for the rectangular geometries typically found at coastal settings, we propose to leverage the wave pressure directly that corresponds to the experimental pressure measurements for different characteristic waves (i.e., wave height, period and surge elevation). Thus, the stochastic process corresponds to the pressure tap measurements at different heights (i.e.,  $S_p^{wave}(t) = Q_w(t)$ ). This limits the range of intensity measures for waves to the tested conditions. However, similar challenges are faced during CFD modeling considering the limited simulated sea states restricted by computational resources. **Error! Reference source not found.** illustrates a wave pressure profile, histogram and time history for breaking waves.

Existing analytical frameworks for determining wave pressures for inland structures such as wave walls are aimed at predicting extreme wave pressure profiles mainly for design purposes rather than for reliability assessments. The renowned Goda equations and the successive modifications are models to estimate peak wave pressure that often overestimate the pressure for conservative purposes. Alternatively, the ASCE 7 also provides guidance for estimating design loads from *breaking* wave pressure. [7] found that the ASCE was very conservative in its predictions. However, the presented analytical models lack the time dependent evolution of

the phenomena which makes a bigger challenge when analyzing winds and waves simultaneously. Therefore, the proposed method can be used to evaluate simultaneous occurrence of wind and waves and evaluate the performance of the building and components in a time-dependent fashion accounting for progressive damages.

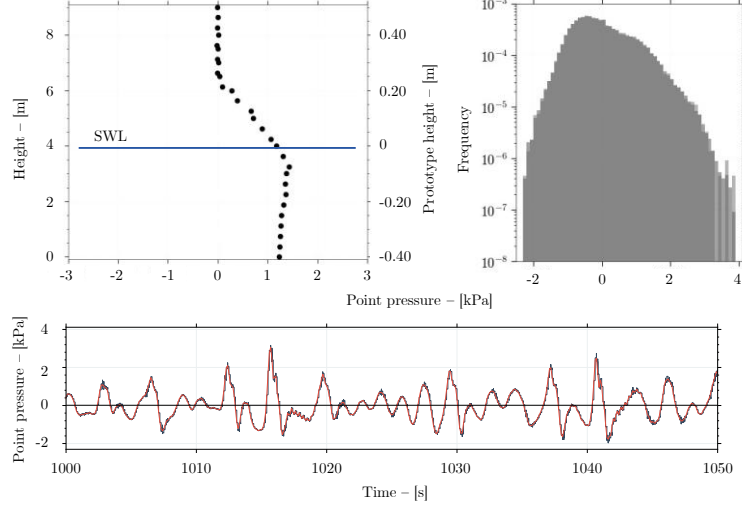


**Figure 3:** Wave pressure profile, pressure frequency distribution and time histories for breaking waves

The loads considered from the surge correspond to the hydrostatic pressure that results from the water elevation and the hydrodynamic pressure resulting from the water velocity. The hydrostatic linear pressure profile is calculated from Eq.4 and is applied to all the building sides equally. Vertical hydrostatic flotation pressure is neglected.

$$Q_H^{(k)}(t; \mathbf{IM}, \mathbf{X}) = \rho_w g h^{(k)}(t; \mathbf{IM}, \mathbf{X}) \quad (4)$$

where  $Q_H^{(k)}(t; \mathbf{IM}, \mathbf{X})$  = hydrostatic pressure at point  $k$  for the surge elevation  $H_S$  contained in  $\mathbf{IM}$  and parameters  $\mathbf{X}$ .  $\rho_w$  = water density,  $g$  = gravity constant and  $h^{(k)}(t; \mathbf{IM}, \mathbf{X})$  = water elevation at point  $k$ .

The hydrodynamic surge pressure derived from the current velocity is treated as a deterministic process considering that this pressure has minimal time-dependent variation and its secondary to the wave loads [14]. Therefore, the surge velocity pressure is derived as shown in Eq.5. The pressure coefficient  $C_V$  and the current velocity are treated deterministically based on the recommendations from FEMA P-259. The  $C_V$  was determined based on the building's width/length ratio.

$$Q_V^{(k)}(t; \mathbf{IM}, \mathbf{X}) = \frac{1}{2} \rho_w C_V V(\mathbf{IM})^2 \quad (5)$$

where  $Q_V$  = hydrodynamic pressure at point  $k$  estimated for surge elevation  $H_S$  contained in  $\mathbf{IM}$  and parameters  $\mathbf{X}$ .  $C_V$  = dynamic pressure coefficient and  $V$  = surge fluid velocity.

The progressive damage of the roof and walls is used to inform rainfall ingress and interior damage. State-of-the-art CFD models have been explored to determine the amount of water ingress, however, in the present study we propose only to consider the potential damage from rainfall as a function of the amount of damage of the roof panels. Further work can focus on determining the amount of water ingress and damage estimation of the interior.

The progressive damage of the roof and walls is used to inform rainfall ingress and interior damage. State-of-the-art CFD models have been explored to determine the amount of water ingress, however, in the present study we propose only to consider the potential damage from rainfall as a function of the amount of damage of the roof panels. Further work can focus on determining the amount of water ingress and damage estimation of the interior.

### 2.3 Intensity measure vector

The multi-hazard intensity measure vector considers wind, waves, storm surges, and rainfall. The wind measure is the 3-s peak gust wind velocity  $U$  that is aligned with ASCE 7 and multiple catastrophe modeling approaches. When informed by wind tunnel test, the reference wind velocity is usually taken at mid-roof level, therefore an exposure-dependent wind velocity profile is needed to relate the velocities. TC wind velocities at coastal shores are explored in the 0 to 150 m/s velocity range, that is, up to category V in the Saffir-Simpson scale. The waves considered in the analysis are determined by the available experimental data from the wave flume test [9]. Therefore, the intensities considered to characterize the waves are the wave height  $H_w$  and wave period  $T_w$ . The significant wave height  $H_{1/3}$  and peak period  $T_p$  for irregular waves and mean wave height  $\bar{H}$  and mean period  $\bar{T}_w$  for regular waves. For both wave heights, the  $IM$  varied from 1 to 5 m and the periods vary from 2.52-s to 5.04-s.

The surge elevation  $H_s$  for the large wave flume tests was set in 4 m at the location of the building structure (i.e., water sea level WSL). However, we used a variable surge elevation for this  $IM$  by assuming different elevations for the building base. Hence the relative flood elevation changes. This assumption neglects the behavior change of wave pressure for lower or higher water elevations. However, it is a conservative assumption for lower than 4 m surge heights. Similarly, for most model geometries, the height of the building exposed to waves is very limited for elevations higher than 4 m. The  $H_s$  range was set between 0 and 8 m based on ACIRC+SWAN simulations for the industrial corridor of the Houston Ship Channel considering FEMA033 and FEMA036 synthetic storms [15]. The hydrostatic and hydrodynamic pressures were calculated using  $H_s$ . For the latter pressure, the ranges for current velocities were set from 0 to 5 m/s to account for low and high flow velocities.

### 2.4 Multi-hazard loading

The loads are applied in the following order: first the surge elevation for the time  $t$  is recorded and the hydrostatic and hydrodynamic forces are estimated. Then the wave pressure profile for that time step added and applied to the structure's envelope considering the relative surge elevation. The instantaneous wind pressure is applied last for all the surface above surge elevation where the wave pressure is negligible. This proposed loading method does not account for wave-wind interactions and ignores the local changes in wind pressure due to the presence of the wave. However, it does account for the explicit occurrence of all the hazards spatially and temporarily. Hence, it is unnecessary to use a joint probability density function that is challenging to characterize. Similarly, there is no need to calibrate or determine factors to account for joint peak pressures. **Error! Reference source not found.** illustrates the proposed multi-hazard loading.

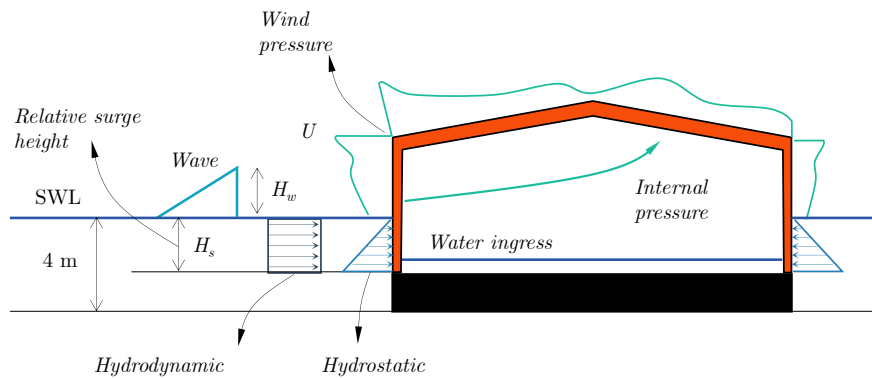


**Figure 4:** Schematic multi-hazard model loads at time instant  $t$

## 2.5 Time dependent reliability assessment

The envelope components, structural elements and system-level reliability assessment are performed in a time dependent yet quasi-static fashion. The dominant frequencies for wind and waves excitations are not resonant to natural frequencies of portal frames that are light and stiff structures. Therefore, a small dynamic fluid-structure interaction is expected as evidenced by [9] in the wave tests. Similarly, experimental analysis suggests that the wind dynamic response is not relevant for envelope components such as cladding panels and fasteners. Additionally, time dependent responses such as low-cycle fatigue can be propagated by modifying the capacity of the components.

The time dependent analysis allows for account for damage accumulation, progressive damage sequences such as flood ingress and internal wind pressurization and modifying the transferred loads along the load path. The total damage informs the fragility for the envelope and structural systems within a Monte Carlo simulation framework. Water ingress and internal wind pressurization modifies the loads and damage states of the structure. The contents that are vulnerable to water are expected to be heavily damage is surge ingresses the building. Similarly, internal wind pressure leads to extreme uplift pressure that results in extensive roof covering damage and secondary structure failure (e.g., purlin buckling). Finally, the failure of components along the loading path modifies the transferred loads between systems. For instance, the failure of wall cladding makes it incapable to carry the wave or wind pressures, therefore such loads are not transmitted (or partially transmitted) to the supporting structure (e.g. girt or purlin). This process accounts for realistic damage progression that better informs component-level and system-level fragilities.

## 2.6 Multi-fidelity models

Multiple analysis models can be chained together to perform the quasi-static time dependent reliability analysis. For the envelope, wall and roof panels are proposed to be modeled to accommodate spatially varying pressure, therefore, a FEM model was used to estimate the demands on the panel and its connections. However for components such as overhead doors, windows and other fenestrations with limited data, probabilistic models for the pressure capacity can be used instead to evaluate the time-step performance. Similarly, for supporting structures such as purlins and girts, 1D linear analysis can be used to estimate the demand and



evaluate the occurrence of different failure modes. In contrast, for the main frames (end- or middle) that determine the system level performance (e.g., bay collapse), a fiber-based nonlinear OpenSees [16] model was leveraged to analyzed the response.

## 2.6 Design of experiments

A design of experiments (DoE) is assemble to represent multiple prototypes of the portal frame structures and propagate uncertainty. The geometry layout (i.e., width, length, height and roof slope) is informed by the wind tunnel databases to avoid extrapolation and maximize the experimental information. Multiple design levels are considered for the cross-sectional properties of frame and supporting structures. The material properties are treated as deterministic considering the low uncertainty in the steel construction. The envelope components (i.e., cladding panels) considered are R-panels with deterministic materiality and geometry. The uncertainty in the pressure capacity is considered in the fasteners that are subjected to extreme wind uplift pressure and can be affected by time dependent deterioration such as corrosion and low cycle fatigue. A smart sampling strategy is used to meet a certain variability in the resulting fragilities within a Monte Carlo simulation framework (i.e., Monte Carlo stopping rule). First, Latin hypercube sampling is used to define a large sample space for the DoE. Then, samples are simulated while monitoring for the coefficient of variation in the fragility at a certain intensity measure vector  $\mathbf{im}$  threshold. Eq. 6 shows the fragility estimator and Eq.7. the stopping rule based on Bernoulli trials.

$$\hat{P}(DS = ds|\mathbf{im}, \boldsymbol{\theta}, \mathbf{X}) = \frac{1}{N_{MC}^{(i)}} \sum_{j=1}^{N_{MC}^{(i)}} \mathbb{I}_{ds}(\{\mathbf{im}, \boldsymbol{\theta}, \mathbf{X}\}^j) \quad (6)$$

$$N_{MC}^{(i+1)} = \frac{1 - \hat{P}(DS = ds|\mathbf{im}, \boldsymbol{\theta}, \mathbf{X})}{\delta^2 \hat{P}(DS = ds|\mathbf{im}, \boldsymbol{\theta}, \mathbf{X})} \quad (7)$$

where  $\hat{P}(DS = ds|\mathbf{im}, \boldsymbol{\theta}, \mathbf{X})$  = estimator for the damage state probability conditioned on a given realization of the intensity measure  $im$ , hazard and structure properties  $\boldsymbol{\theta}$  and  $\mathbf{X}$  respectively.  $N_{MC}^{(i)}$  and  $N_{MC}^{(i+1)}$  are the number of Monte Carlo simulations at moment  $i$  and  $i + 1$ , respectively.  $\mathbb{I}_{ds}(\{\mathbf{im}, \boldsymbol{\theta}, \mathbf{X}\}^j)$  = indicator function for the damage state  $ds$  and the  $j$ -th sample.  $\delta$  = coefficient of variation as target confidence level.

## 2.7 Fragility analysis and surrogate model

The results of the time-dependent reliability analysis are used to inform failure and damage extent probabilities conditioned on the intensity measures vector  $\mathbf{IM}$  and key parameters that help to characterize the portal frame structures as a class. The parametrization is performed for geometric characteristics (e.g., height, roof slope or area) and design levels. To account for damage extent, damage states are proposed to classify the simulation outcome. The damage states are highly related to the functionality loss and recovery processes. Surrogate modeling is used to generalize the input-output information informed by the DoE and Monte Carlo simulations, respectively. Multi-dimensional machine learning regression techniques are leveraged as surrogates to derive close form fragility functions as shown in Eq.8.

$$P(DS \geq ds | \mathbf{IM}, \boldsymbol{\theta}, \mathbf{X}) = f \left( \sum_{i=1}^{N_{im}} \beta_i \mathbf{IM}^{(i)} + \beta_{\theta} \boldsymbol{\theta} + \beta_x \mathbf{X} + \beta_o \right) \quad (8)$$

where  $P(DS \geq ds | \mathbf{IM}, \boldsymbol{\theta}, \mathbf{X})$  = the multi-parametric fragility model and  $f(\cdot)$  is the surrogate model.  $N_{im}$  = number of intensity measures,  $\boldsymbol{\beta} = \{\beta_{IM}, \beta_{\theta}, \beta_x, \beta_o\}$  are the regression model coefficients.

### 3 CASE STUDY

#### 3.1 Portal frame structures

The portal frame structures typically found in industrial settings such as petrochemical, manufacturing and power plants facilities are used as case studies. A multiple of these structures can be found in a single facility for storage (e.g., warehouses) and production uses. The main structure supporting gravitational and in-plane lateral loads are the single-bay moment resistant frames often found in tapered cross-sections. Bracing is used for supporting frames out-of-plane lateral loads and diaphragm loads at roof level. Secondary structures such as purlins and girts are used to support the envelope system consisting of wall and roof cladding. Metal cladding is often used in industrial settings for its longevity. One typology widely used is the fastener-exposed rib metal cladding, the R-Panel for both roofs and walls. However, there is a large variety of cladding systems. Additional components include windows, doors and overhead access doors. The foundation consists of anchored columns based on metal plates connected to concrete pedestals or slabs.

Cladding components are expected to fail due to fastener failure (pull-out), panel fracture at fastener zones (uplift pressure) and bending under positive pressure. Secondary cold-formed steel C or Z profile structure can experience buckling and bending failure. The moment frames failure modes are flexural and base connection failure. However, end bay frames are more likely to fail due to limited out-of-plane support but most importantly for their different structural layout that allows accommodating fenestrations and add flexibility to expansion projects in the future. The fenestrations, especially the overhead doors, can fail and lead to important internal pressure.

#### 3.2 Heterogenous portfolios

The portal frame structures of the Houston Ship Channel (HSC) in the Texas US Gulf coast are used as a testbed to assess the fragility of large and heterogenous portfolios. The HSC is a house of multiple industrial facilities including major refineries and petrochemical facilities. A survey was conducted to determine the number of portal frame structures in the industrial corridor. A total of 1500 industrial warehouses and industrial buildings were identified that are likely to have a portal frame structural system.

### 4 CONCLUSIONS

The proposed framework contributes to the estimation of multi-hazard tropical cyclone fragilities. The major contribution corresponds to the explicit multi-physics time dependent simulation of wind, waves, surges and rainfall. Different to the existing methodologies, this analytical framework allows us to accommodate surge, wave and wind loads simultaneously while representing the spatio-temporal variation of the acting pressures. By representing the

pressure stochastically, the uncertainty of the intensity measures is captured directly in the analysis. Therefore, no assumptions on the occurrence of peak loads, spatial distribution, correlation structure must take place. Additionally, the framework allows progressive damage and damage sequences such as internal pressurization, internal flooding and rainwater ingress. Furthermore, it permits to simulate the transferred load from an envelope system to the structural system accounting for the performance of individual components.

Different to CFD simulation that uses a well-established power spectrum to generate TC hazard intensity measures, the proposed analytical method leverages existing experimental data to inform structure-specific power spectrums of the response. A spectral representation method can then be used to generate the time histories of the intensity measures while preserving multi-point coherence and correlation. The framework uses a case study of a portal frame structure typically found in industrial settings to estimate multiple damage state fragilities. Additionally, it also uses a large portfolio of these structures as a testbed to demonstrate the capacity of the method to account for heterogeneous structures.

Further work is intended to compare the present framework against other existing analytical methods and also with CFD simulations. Further efforts should focus on understanding the particular physical interaction between stressors in a time dependent fashion to incorporate into the analysis. It is expected that the present study can help find an intermediate fidelity between code-based reliability analysis and complex CFD simulations while leveraging and assimilating existing and new experimental data.

## REFERENCES

- [1] M. Amini and A. M. Memari, "CFD-Based Evaluation of Elevated Coastal Residential Buildings under Hurricane Wind Loads," *Journal of Architectural Engineering*, vol. 27, no. 3, p. 04021014, Sep. 2021, doi: 10.1061/(ASCE)AE.1943-5568.0000472.
- [2] M. Moeini and A. M. Memari, "Hurricane-Induced Failure Mechanisms in Low-Rise Residential Buildings and Future Research Directions," *Natural Hazards Review*, vol. 24, no. 2, p. 03123001, May 2023, doi: 10.1061/NHREFO.NHENG-1544.
- [3] O. M. Nofal *et al.*, "Methodology for Regional Multihazard Hurricane Damage and Risk Assessment," *Journal of Structural Engineering*, vol. 147, no. 11, p. 04021185, Nov. 2021, doi: 10.1061/(ASCE)ST.1943-541X.0003144.
- [4] W. Cui and L. Caracoglia, "Performance-Based Wind Engineering of Tall Buildings Examining Life-Cycle Downtime and Multisource Wind Damage," *Journal of Structural Engineering*, vol. 146, no. 1, p. 04019179, Jan. 2020, doi: 10.1061/(ASCE)ST.1943-541X.0002479.
- [5] K. A. Porter, A. S. Kiremidjian, and J. S. LeGrue, "Assembly-Based Vulnerability of Buildings and Its Use in Performance Evaluation," *Earthquake Spectra*, vol. 17, no. 2, pp. 291–312, May 2001, doi: 10.1193/1.1586176.
- [6] Z. Ding, W. Zhang, W. Hughes, and D. Zhu, "A modified sub-assembly approach for hurricane induced wind-surge-wave vulnerability assessment of low-rise wood buildings in coastal communities," *Journal of Wind Engineering and Industrial Aerodynamics*, vol. 218, p. 104755, Nov. 2021, doi: 10.1016/j.jweia.2021.104755.
- [7] T. Tomiczek, A. Wyman, H. Park, and D. T. Cox, "Modified Goda Equations to Predict Pressure Distribution and Horizontal Forces for Design of Elevated Coastal Structures,"

- Journal of Waterway, Port, Coastal, and Ocean Engineering*, vol. 145, no. 6, p. 04019023, Nov. 2019, doi: 10.1061/(ASCE)WW.1943-5460.0000527.
- [8] Y. Quan, Y. Tamura, M. Matsui, S. Y. Cao, and A. Yoshida, “TPU aerodynamic database for low-rise buildings,” *Proceedings of 12th International Conference on Wind Engineering*, pp. 1615–1622, Jan. 2007.
- [9] H. Park, T. Tomiczek, D. T. Cox, J. W. van de Lindt, and P. Lomonaco, “Experimental modeling of horizontal and vertical wave forces on an elevated coastal structure,” *Coastal Engineering*, vol. 128, pp. 58–74, Oct. 2017, doi: 10.1016/j.coastaleng.2017.08.001.
- [10] X. Chen and A. Kareem, “Proper Orthogonal Decomposition-Based Modeling, Analysis, and Simulation of Dynamic Wind Load Effects on Structures,” *Journal of Engineering Mechanics*, vol. 131, no. 4, pp. 325–339, Apr. 2005, doi: 10.1061/(ASCE)0733-9399(2005)131:4(325).
- [11] M. Grigoriu, *Applied non-Gaussian processes: examples, theory, simulation, linear random vibration, and MATLAB solutions*, 1. print. Englewood Cliffs, N.J: PTR Prentice Hall, 1995.
- [12] G. Cuomo, W. Allsop, T. Bruce, and J. Pearson, “Breaking wave loads at vertical seawalls and breakwaters,” *Coastal Engineering*, vol. 57, no. 4, pp. 424–439, Apr. 2010, doi: 10.1016/j.coastaleng.2009.11.005.
- [13] C. Kafali and M. Grigoriu, “System Performance Under Multi-Hazard Environments”.
- [14] C. Bernier and J. E. Padgett, “Buckling of aboveground storage tanks subjected to storm surge and wave loads,” *Engineering Structures*, vol. 197, p. 109388, Oct. 2019, doi: 10.1016/j.engstruct.2019.109388.
- [15] B. Ebersole *et al.*, “Interim report—Ike Dike concept for reducing hurricane storm surge in the Houston-Galveston region,” *Jackson State Univ. Accessed December*, vol. 12, p. 2016, 2015.
- [16] F. McKenna, M. H. Scott, and G. L. Fenves, “Nonlinear Finite-Element Analysis Software Architecture Using Object Composition,” *Journal of Computing in Civil Engineering*, vol. 24, no. 1, pp. 95–107, Jan. 2010, doi: 10.1061/(ASCE)CP.1943-5487.0000002.